Current Research in Food Science 5 (2022) 1965–1975

Contents lists available at ScienceDirect

Current Research in Food Science

journal homepage: www.sciencedirect.com/journal/current-research-in-food-science

Characteristics and osteogenic mechanism of glycosylated peptides-calcium chelate

Xiaoping Wu [a,b], Fangfang Wang [b], Xixi Cai [b,**], Shaoyun Wang [b,*]

[a] College of Chemical Engineering, Fuzhou University, Fuzhou, 350108, China
[b] College of Biological Science and Engineering, Fuzhou University, Fuzhou, 350108, China

ARTICLE INFO

Keywords:
Peptide-calcium chelate
Glycosylation
Structural properties
Osteogenic activity
Wnt/β-catenin signaling pathway

ABSTRACT

Finding effective practical components to promote bone mineralization from the diet has become an effective method to regulate bone mass. In this study, peptides-calcium chelate derived from Crimson Snapper scales protein hydrolysates (CSPHs), and xylooligosaccharide (XOS)-peptides-calcium chelate prepared by transglutaminase (TGase) pathway, named CSPHs-Ca and XOS-CSPHs-Ca-TG, were used to explore the effects of glycosylation on their structural properties and osteogenic activity *in vitro*. Results showed that XOS-CSPHs-Ca-TG had better calcium phosphate crystallization inhibition activity with more unified structures than CSPHs-Ca, and could effectively maintain a stable calcium content in the gastrointestinal tract. Meanwhile, the glycosylated peptide-calcium chelate could accelerate the calcium transport efficiency in the Caco-2 cell monolayer, up to 3.54 folds of the control group. Moreover, XOS-CSPHs-Ca-TG exhibited prominent osteogenic effects by promoting the proliferation of MC3T3-E1 cells, increasing the secretion of osteogenic related factors, and accelerating the formation of intracellular mineralized nodules. RT-qPCR results further confirmed that this beneficial effect of XOS-CSPHs-Ca-TG was achieved by activating the Wnt/β-catenin signaling pathway. These results suggested that glycosylation might be a promising method for optimizing structural properties and osteogenic activity of peptide-calcium chelate.

1. Introduction

Osteoporosis is one of the most common bone diseases and stands sixth among the most frequently-occurring diseases. Its clinical manifestations are reduced bone mass, destruction of bone microstructure, and increased bone brittleness, leading to increased fracture risk (Wu et al., 2020). Bone remodeling is achieved by coordinating two cell types with opposite functions, namely osteoclasts and osteoblasts (Zhang et al., 2021). Regularly, bone formation of osteoblasts and resorption of osteoclasts are in a dynamic balance during bone reconstruction. When both values change and tend to resorption, osteoporosis will occur (Jie et al., 2018). Currently, the treatment of osteoporosis is still based on chemical drugs. According to the different action mechanisms, they can be divided into bone resorption inhibitors (bisphosphonates, estrogen, calcitonin), bone formation promoters (fluoride, strontium preparations), and bone mineralization drugs (Vitamin D, calcium preparations). However, various side effects and high costs limit the application of the first two treatments (Tonk et al., 2022). Therefore, finding practical components to promote bone mineralization will be an efficient way to regulate bone mass.

Calcium is the main component of human bones and teeth, 90% of which is absorbed in the small intestine. However, in the weak alkaline environment of the small intestine, calcium ions are inclined to form insoluble calcium salt with acid radical ions in food, leading to the reduction of calcium bioavailability in the human body (Gao et al., 2018a). Therefore, novel calcium supplements emerged as the time required, among which peptides like casein phosphopeptide (CPP) (Liu et al., 2021) and phosvitin phosphopeptide (PPP) (Jiang and Mine, 2000) are the prominent representatives. They can combine calcium ions to prevent precipitation, thus increasing soluble calcium concentration in the small intestine (Zhu et al., 2020). Additionally, as the primary calcium carrier, they can interact with the cell membrane and then open the calcium channel to promote calcium absorption in the human body to ameliorate osteoporosis (Lin et al., 2020). Recent studies have demonstrated that peptides extracted from egg yolk soluble protein (Kim et al., 2008), fish collagen (Yamada et al., 2013), and bovine serum

* Corresponding author.
** Corresponding author.
E-mail addresses: caixx@fzu.edu.cn (X. Cai), shywang@fzu.edu.cn (S. Wang).

https://doi.org/10.1016/j.crfs.2022.10.008
Received 28 June 2022; Received in revised form 9 September 2022; Accepted 6 October 2022
Available online 17 October 2022

(Liu et al., 2014) could promote calcium absorption and have osteoprotective activity by inducing the differentiation of pre-osteoblasts. Further studies showed that porcine bone collagen peptide-calcium chelate could up-regulate the expression of osteoblast differentiation markers, such as alkaline phosphatase, type I collagen, and Runx2 (Wu et al., 2020). Zhang et al. (2018a) found that the bone mineral density and bone strength of ovariectomized rats fed with Pacific cod peptide-calcium chelate were significantly increased. Similar results were also obtained in the bone metabolism of collagen peptide-calcium chelate in rats with calcium deficiency models by Zhao et al. (2014) and Wang et al. (2018a). These results suggest that peptide-calcium chelate benefits bone metabolism and could be a potential supplement for improving osteoporosis.

Indigestible oligosaccharides are considered the most promising prebiotics for bone health because they can stimulate and activate intestinal flora, promote calcium absorption, improve bone strength and benefit other bone health agents (Arora et al., 2021). Zhang et al. (2021) found that FOS/GOS could significantly improve bone loss in mice. By feeding calcium deficient mice with Konjac oligosaccharide for 8 weeks, Ai et al. (2021) found that the number of trabeculae and bone mechanical strength was heightened. Therefore, indigestible oligosaccharides are also considered a new substance to improve osteoporosis. Moreover, glycosylation is the most common way of protein chemical modification. Based on the advantage of glycosylation modification and the in-depth study of functional peptides, glycosylation has been applied to peptides to improve their physiological activity (Gao et al., 2018b). Zhu et al. (2020) investigated the fabrication of calcium delivery systems by casein phosphopeptides and chitosan oligosaccharides, showing that the delivery vehicles could enhance calcium retention and bone synthesis in mice. However, the knowledge of the mechanism of glycosylated peptide-calcium chelate promoting bone formation is still limited.

Therefore, in the present study, novel glycosylated peptide-calcium chelates derived from Crimson Snapper scales protein hydrolysates (CSPHs) and xylooligosaccharide (XOS) were prepared, and their calcium absorption promoting activity was investigated in the Caco-2 cell model. In addition, the osteogenesis effects and the underlying mechanism of the prepared peptide-calcium chelates were evaluated in the MC3T3-E1 cell model. These results could provide theoretical support for the potential application of peptide-calcium chelates in bone metabolism.

2. Materials and methods

2.1. Materials

Crimson Snapper scales were provided by Putian Haiyibai Co., Ltd. (Fujian, China). XOS, propidium iodide (PI), and transglutaminase (TGase) were purchased from Shanghai Yuanye Biological Technology Co., Ltd. (Shanghai, China). DMEM medium, α-MEM medium, Hank's balanced salt solution (HBSS), non-essential amino acids, and penicillin/streptomycin solution were purchased from Dalian Meilun Biotechnology Co., Ltd. (Dalian, China). Fetal bovine serum (FBS) was purchased from NEWZERUM Ltd. (Christchurch, New Zealand). β-glycerophosphate was the product of Sigma Aldrich (St. Louis, Missouri, USA). DKK 1 was the product of APExBIO Technology LLC (Houston, USA). Caco-2 cells and MC3T3-E1 cells were obtained from BeNa Culture Collection (Kunshan, China). Alkaline phosphatase (ALP), osteocalcin (OCN), and type I collagen (Col-I) enzyme-linked immunosorbent assay (ELISA) kits were the products of Nanjing Jiancheng Bioengineering Institute (Nanjing, China). Fluo-3AM was purchased from Beyotime Biotechnology Co., Ltd. (Shanghai, China). All other chemicals and reagents were of analytical grade and commercially available.

2.2. Preparation of crimson snapper scales protein hydrolysates

The scales were dispersed in distilled water (4%, m/V) and autoclaved for 60 min. Before the addition of flavourzyme (E:S = 1:25), the pH value of the mixture was adjusted to 6.30. After being hydrolyzed at 50 °C for 9 h, the hydrolysate was immersed in boiling water for 10 min to inactivate the enzyme. The degree of hydrolysis was 18.21% by formaldehyde titration (Li et al., 2012). Subsequently, the mixture was centrifuged at 10,000 rpm for 20 min, and then the supernatant was collected and freeze-dried. The resulting powder was identified as CSPHs.

2.3. Preparation of glycosylated peptide copolymers by TGase

The mass ratio of XOS to CSPHs was 1:0.85, and the total concentration was 30 mg/mL by adding distilled water. Before adding TGase (E:S = 1:10) to the mixture, the pH value of the solution was adjusted to 6.00. Then, the mixture solution was stirred in a water bath for 1.5 h at 40 °C. After that, the complete solution was heated at 95 °C for 10 min to inactivate the enzyme. Then, the solution was cooled to room temperature, put into a dialysis bag, and dialyzed at 20 °C for 24 h (Zhao et al., 2014). Finally, the resulting product was lyophilized. The grafting degree of the freeze-dried powder was 55.62%, calculated by the ortho-phthalaldehyde (OPA) method (Pirestani et al., 2017), and was named XOS-CSPHs-TG.

CSPHs and XOS-CSPHs-TG were respectively dispersed in distilled water to a concentration of 20 mg/mL (pH 7.50). Solid $CaCl_2$ was added to obtain a samples/$CaCl_2$ mixture with a mass ratio of 5:1. Then, the mixtures were held at 30 °C for 20 min. To obtain CSPHs and XOS-CSPHs-TG calcium chelates, anhydrous ethanol was added to the mixtures and centrifuged at 10,000 rpm for 20 min. After the precipitates were lyophilized, their calcium-binding rate was determined to be 87.43% and 91.29%, according to the method of Zhang, Lin and Wang (2018b), respectively, which were defined as CSPHs-Ca and XOS-CSPHs-Ca-TG.

2.4. Properties and structural characterization of calcium chelating peptides

2.4.1. Inhibition of calcium phosphate crystallization

Each of CSPHs and XOS-CSPHs-TG (20 mg) was dissolved in 2 mL of 0.8 M $CaCl_2$ solution (pH 7.00) and maintained at 37 °C for 5 min, respectively. Subsequently, 0.008 M NaH_2PO_4 (200 mL) was added to the solution. The decreasing pH of the solution was recorded every 5 min for 30 min. Distilled water was used as blank control and EDTA as a positive control.

2.4.2. Simulated gastrointestinal digestion experiments

The prepared 1 mg/mL pepsin solution (pH 2.00) and 1 mg/mL pancreatin solution (pH 7.00) were used to simulate the gastric and intestinal fluid. CSPHs-Ca and XOS-CSPHs-Ca-TG were dissolved in distilled water (0.5 mg/mL), respectively, and the pH of the solutions was adjusted to 2.00. After that, 1 mg/mL pepsin solution was added to make the mass ratio of enzyme to chelates 1:50 and was subsequently magnetic stirred at 37 °C for 2 h. Then, the solution was adjusted to pH 7.00 and added with 1 mg/mL trypsin solution to make the mass ratio of enzyme to sample 1:25, followed by maintaining at 37 °C for 2 h with magnetic stirring. During which, 1 mL of solution was taken out every 30 min to calculate the calcium ions retention rate as follows:

$$\text{The calcium retention profile } (\%) = \frac{M_0}{M} \times 100\% \quad (1)$$

M (g) was the total calcium content in samples, and M_0 (g) was the calcium content in samples.

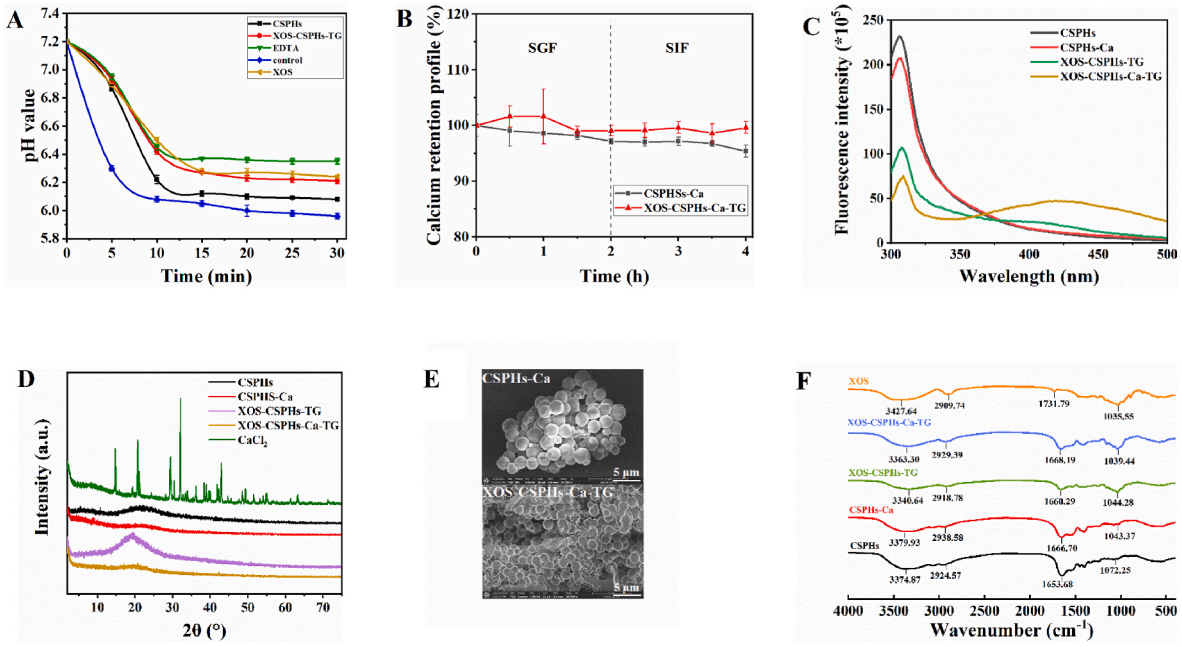

Fig. 1. Characterization of the structure and properties of CSPHs-Ca and XOS-CSPHs-Ca-TG. (A) Inhibition of calcium phosphate crystallization. (B) Calcium retention profile. (C) Fluorescence spectrum. (D) XRD patterns. (E) Scanning electron microscope (SEM) image at 2000 × magnification. (F) Fourier transform infrared spectrogram (FTIR).

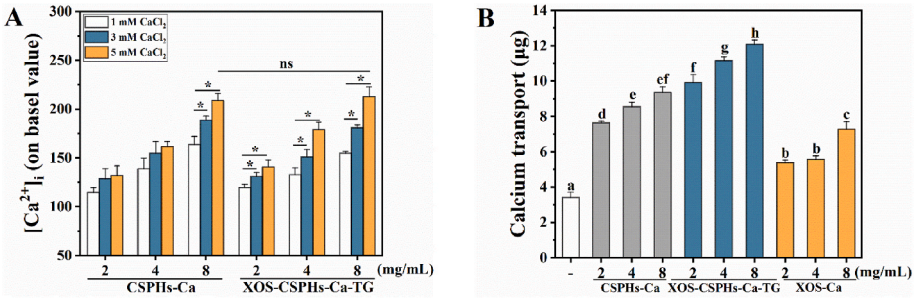

Fig. 2. The absorption promoting effect of CSPHs-Ca and XOS-CSPHs-Ca-TG. (A) Effects on promoting calcium absorption. (B) Effects on calcium transport across Caco-2 monolayers. Different lowercase letters mean a significantly different, $p < 0.05$. "*" represents $p < 0.05$, "ns" represents $p > 0.05$.

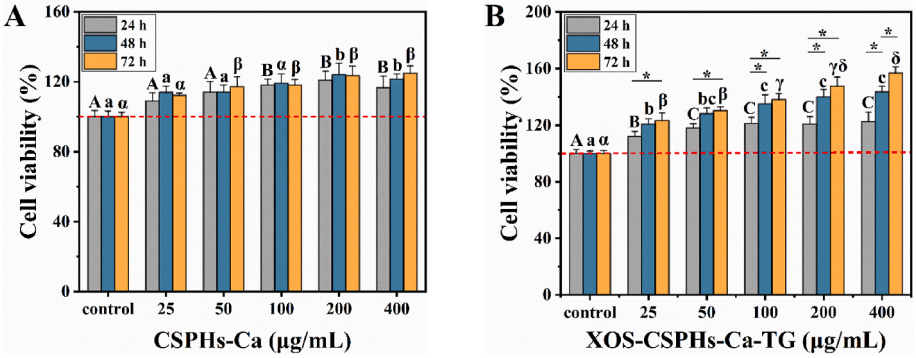

Fig. 3. Effects of CSPHs-Ca (A) and XOS-CSPHs-Ca-TG (B) on the viability of MC3T3-E1 cells. Different letters mean a significantly different, $p < 0.05$. "*" represents $p < 0.05$.

2.4.3. Fourier transform infrared spectroscopy (FTIR)

FTIR images were obtained from lyophilized samples (1 mg) with KBr (100 mg). The FTIR spectra were recorded by an infrared spectrophotometer (Nicolet is50, Thermo Fisher Scientific Co., Ltd, Massachusetts, USA) from 4000 to 400 cm^{-1}.

2.4.4. Scanning electron microscopy (SEM)

The microstructures of the complexes were observed by SEM (Helios G4 CX, FEI Czech Republic S.R.O., Cernovická Terasa, Czech Republic). The different lyophilized samples were smeared onto an aluminium plate with double-sided adhesive carbon tape and operated at a voltage

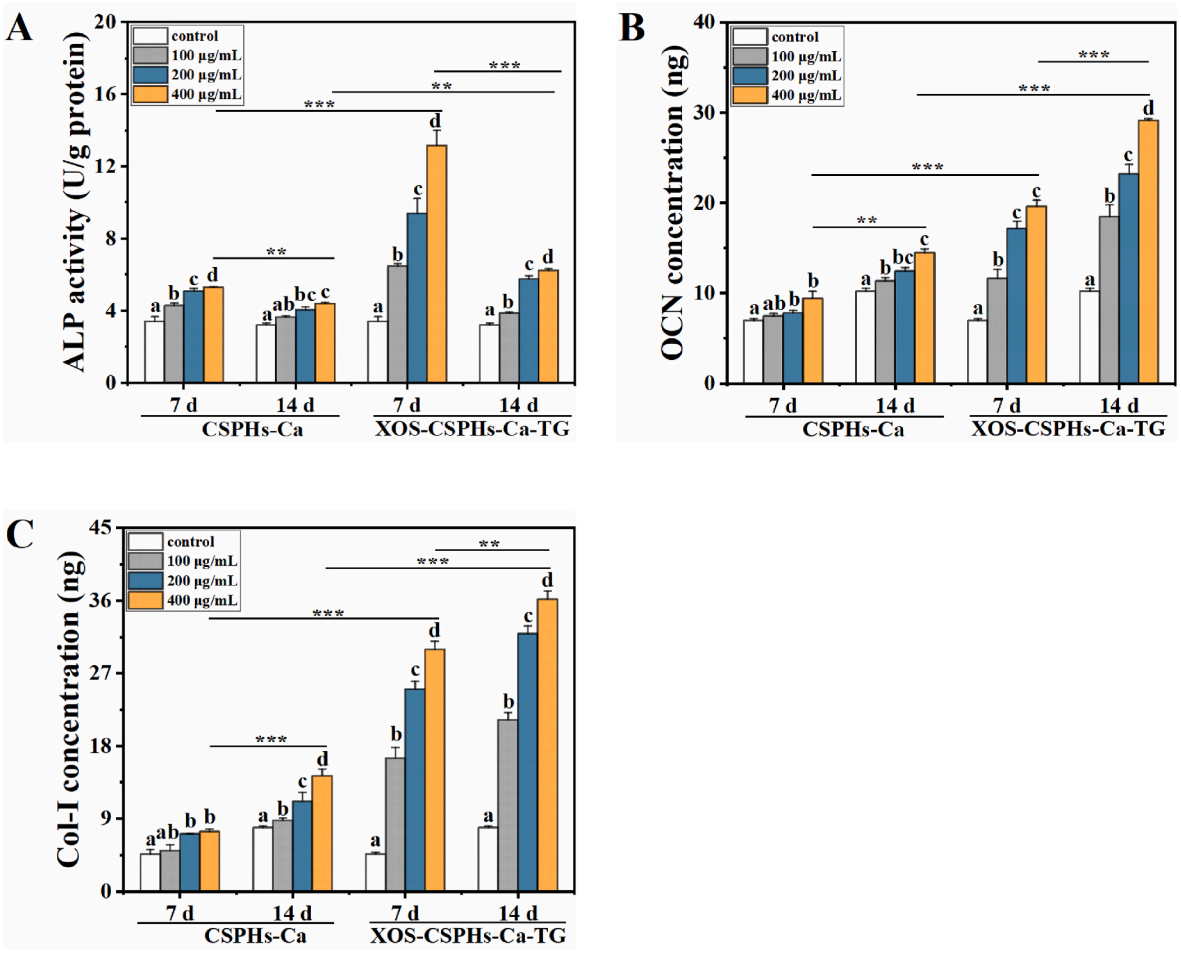

Fig. 4. Effects of CSPHs-Ca and XOS-CSPHs-Ca-TG on the differentiation of MC3T3-E1 cells. (A) Alkaline phosphatase (ALP) activity. (B) Osteocalcin (OCN) secretion. (C) Type I collagen (Col-I) secretion. Different lowercase letters mean a significantly different, $p < 0.05$. "***" represents $p < 0.001$, "**" represents $p < 0.01$.

of 15 kV. Micrographs at 2000 × magnification for subsequent analysis.

2.4.5. Fluorescence spectroscopy analysis

The changes in intrinsic fluorescence were analyzed according to the method of Cai et al. (2015) by a fluorescence spectrometer (Fluoromax-4c-l, Horiba instrument Inc, Piscataway, New Jersey, USA). CSPHs, CSPHs-Ca, XOS-CSPHs-TG, and XOS-CSPHs-Ca-TG were dissolved to 100 μg/mL with deionized water (pH 7.00). The fluorescence spectra were measured at 290–500 nm emission wavelength and 280 nm excitation wavelength, and the slit was 5 nm.

2.4.6. X-ray diffraction (XRD)

The crystal states of $CaCl_2$, XOS-CSPHs-MR, and XOS-CSPHs-Ca-MR were analyzed according to the method of Feng et al. (2022) by an X'pert3 and Empyrean diffractometer (Panalytical, Almelo, Netherlands). Samples were swept continuously over a 2θ range of 2–75° at 4°/min speed.

2.5. Study on calcium absorption promoting activity

2.5.1. Caco-2 cell culture and calcium uptake assay

Caco-2 cells were maintained in DMEM supplemented with 20% (V/V) FBS, 1% non-essential amino acids, and 1% penicillin/streptomycin at 37 °C with 5% CO_2. After reaching 90% confluence, the cells were seeded in 12-well culture dishes (Corning Costar, New York, USA). After incubation for 48 h, cells were treated with CSPHs-Ca and XOS-CSPHs-Ca-TG (2–8 mg/mL) for 2 h, respectively. Subsequently, 100 μL Fluo-3AM (5 μM) was added to each well and incubated at 37 °C for 1 h. Then, 1 mL of HBSS was added to each well and incubated for 30 min. After detached and resuspending with HBSS, the intracellular calcium concentration $[Ca^{2+}]_i$ of the cells was detected by flow cytometry (BD AccuriC6 Plus, BD Bioscience, New Jersey, USA).

2.5.2. Calcium transport assay

Caco-2 cells were seeded on 12-well millicell cell culture inserts (0.4 μm pore size, 12 mm diameter, Corning Costar, New York, USA) for 21 d. The culture medium's volume was 1.5 mL on the basal side and 0.5 mL on the apical side. To evaluate the tight junction permeability of Caco-2 cell monolayer, transepithelial electrical resistance (TEER) values were checked using the Millicell ERS-2 system (Millipore Corporation, Massachusetts, USA). Cell monolayer with a TEER value exceeding 300 Ω cm^{-2} was used for the calcium transport experiments. 4 mg/mL CSPHs-Ca and XOS-CSPHs-Ca-TG were added to the apical side, and then the calcium transport capacity across Caco-2 cell monolayers was measured after 2 h. Finally, the calcium content in the basal side was determined by inductively coupled plasma-atomic emission spectroscopy (Lin et al., 2020) (iCAP7400, Thermo Fisher Scientific, Massachusetts, USA).

2.6. Study on osteogenic activity

2.6.1. MC3T3-E1 cell culture and proliferation experiment

MC3T3-E1 cells were maintained in α-MEM supplemented with 10% (V/V) FBS and 1% penicillin/streptomycin at 37 °C with 5% CO_2. After reaching 90% confluence, the cells were detached and seeded in plastic cell culture clusters (Corning Costar, New York, USA). The α-MEM containing 10 mM β-glycerophosphate and 50 μg/mL ascorbic acid

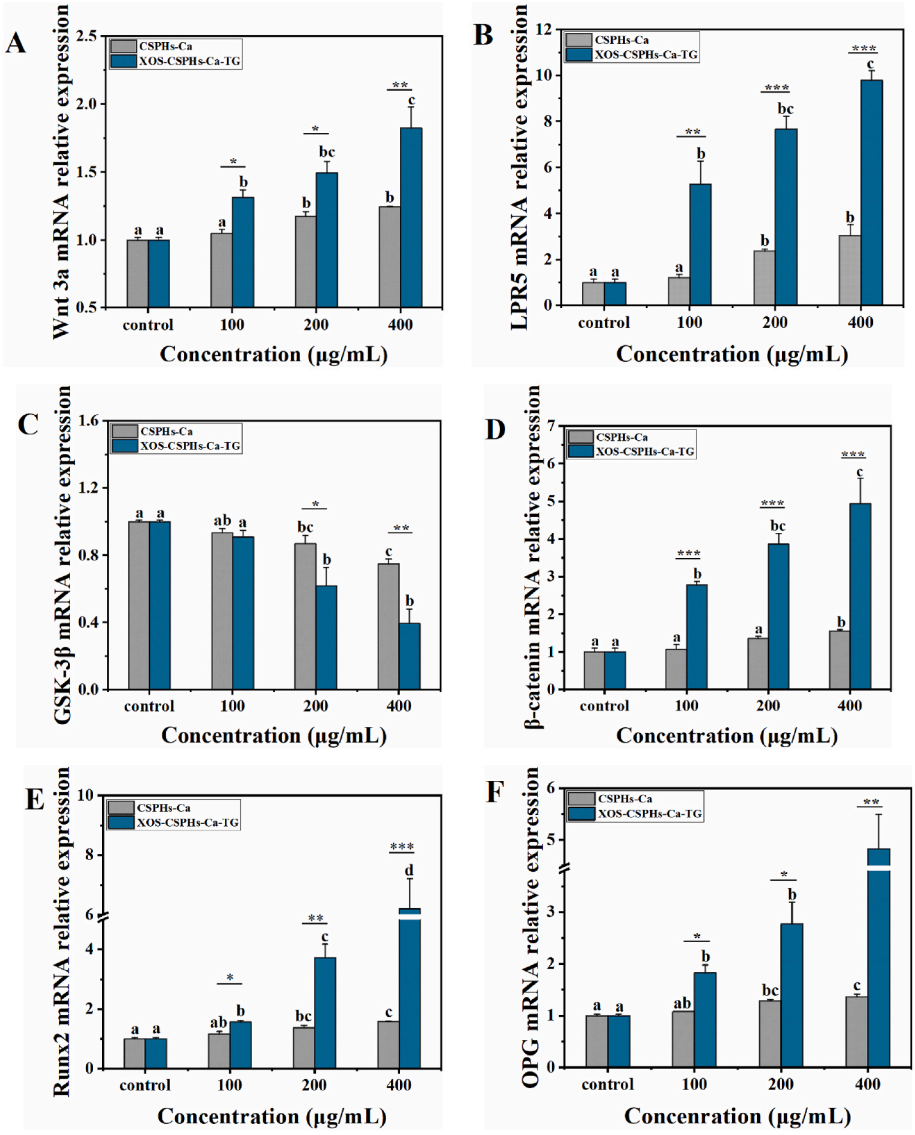

Fig. 5. Effects on mRNA expression of Wnt3a (A), LRP5 (B), GSK-3β (C), β-catenin (D), Runx2 (E), and OPG (F) related to Wnt/β-catenin pathway. Different case letters mean a significantly different, $p<0.05$. "***" represents $p<0.001$, "**" represents $p<0.01$, "*" represents $p<0.05$.

(osteogenic differentiation medium) was used to induce cell differentiation. After 24 h incubation, cells were treated with CSPHs-Ca and XOS-CSPHs-Ca-TG (25–400 μg/mL) for 24–72 h, respectively. Then the cell viability of CSPHs-Ca and XOS-CSPHs-Ca-TG on MC3T3-E1 cells was determined by MTT assay (Wang et al., 2018a).

2.6.2. Cell cycle analysis

MC3T3-E1 cells were treated with CSPHs-Ca and XOS-CSPHs-Ca-TG (100, 200, 400 μg/mL) for 48 h. The cells were collected by centrifugation and fixed with 70% precooled ethanol. 300 μL PI (100 μg/mL) staining solution was added to each tube and stained at 37 °C for 20 min. Then, the fluorescence signal was detected by flow cytometry (BD AccuriC6 Plus, BD Bioscience, New Jersey, USA). The cell cycle was analyzed by ModFit LT software (Verity Software House Inc, Topsham, ME).

2.6.3. ALP enzyme assay

MC3T3-E1 cells were cultured with an osteogenic differentiation medium in the presence of chelates (100, 200, and 400 μg/mL) or DKK 1 (Wnt/β-catenin signal pathway inhibitors) for 7 d and 14 d. After indicated treatment, cells were lysed by repeated freezing and thawing. The lysates were then sonicated in an ice bath for 5 min and centrifuged at 12,000 rpm for 20 min at 4 °C. The intracellular ALP activity and the total protein content were measured, and the measured intracellular ALP activity was standardized by protein concentration.

2.6.4. Measurements of OCN and Col-I secretions by ELISA

MC3T3-E1 cells were cultured with an osteogenic differentiation medium in the presence of chelates for 7 d or 14 d. After differentiation, the supernatants were harvested to determine OCN and Col-I secretions, respectively.

2.6.5. Mineralization assay

MC3T3-E1 cells were seeded in 6-well plates (Corning Costar, New York, USA) and cultured with an osteogenic differentiation medium with chelates or DKK 1 for 21 d. After cultivation, the cells were fixed in 4% (V/V) paraformaldehyde for 10 min. Cells were then stained with Alizarin Red S (pH 4.2, Sigma Aldrich, St. Louis, Missouri, USA) at room temperature for 30 min. After staining, the wells were washed with distilled water to remove the unbound dye, and staining was visualized using microscopy (Ts2, Nikon Instruments Co., Ltd., Tokyo, Japan). To quantify the bound dye, the cells were destained with 10% (V/V)

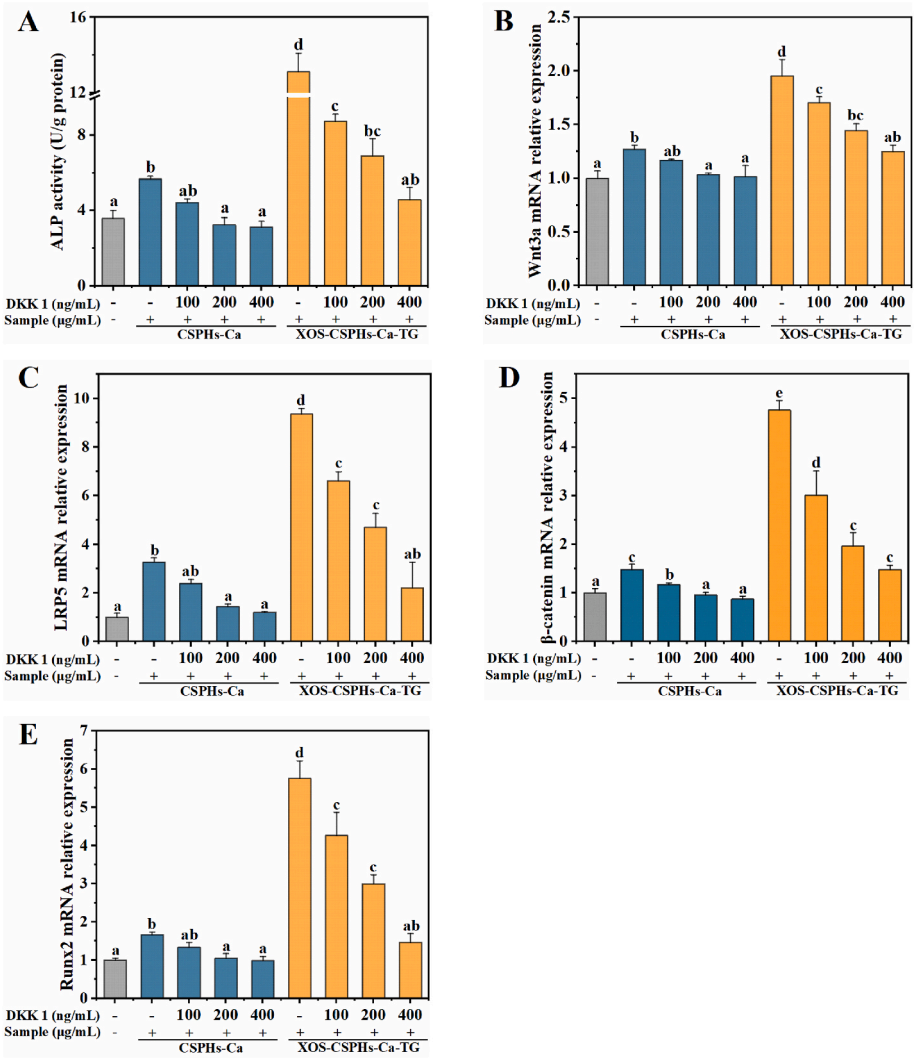

Fig. 6. Effects of Wnt/β-catenin signaling pathway inhibitor DKK 1 on the differentiation of MC3T3-E1 cells. MC3T3-E1 cells were preincubated with various concentrations of DKK 1 for 30 min, followed by CSPHs-Ca and XOS-CSPHs-Ca-TG stimulation. Different lowercase letters mean a significantly different, $p<0.05$.

cetylpyridinium chloride (Shanghai Yuanye Biological Technology Co., Ltd., Shanghai, China) in the dark for 1 h. The solubilized Alizarin Red S concentration was measured at 570 nm using a microplate reader (SpectraMax iD3, Molecular Devices Instrument Co., Ltd., Sunnyvale, USA).

2.6.6. *Quantitative Real-Time Polymerase Chain Reaction (RT-qPCR) analysis*

The MC3T3-E1 cells were treated with an osteogenic differentiation medium with chelates and DKK 1 for 7 d, respectively. Afterward, total RNA was extracted from cells using an RNA preparation pure cell kit (Tiangen Biotechnology Co., Ltd., Beijing, China) and further reverse-transcribed into cDNA using a supermax RT reagent kit with a gDNA eraser (Tansgen Biotech Co., Ltd., Beijing, China). RT-qPCR was performed on a real-time PCR system (Bio-Rad Laboratories, California, USA) after adding the primers and SYBR green I to cDNA. The sequences of the primers were shown in supplemental materials Table S1.

2.7. *Statistical analysis*

All experiments were performed in triplicate, and the resulting values were expressed as means ± standard deviations (SD) and analyzed by one-way analysis of variance (ANOVA) using SPSS 22.0 software (SPSS Inc., Chicago, USA).

3. Results and discussion

3.1. *Properties characterization*

The small molecular weight polypeptides produced by enzymatic hydrolysis of proteins have excellent mineral absorption promoting activity and gastrointestinal stability *in vitro* (Sun et al., 2020). Calcium ion is easy to form insoluble calcium salt with phosphoric acid, phytic acid, and oxalic acid in the intestine, affecting the bioavailability of calcium (Gao et al., 2018b). In the precipitation reaction of Ca^{2+} and PO_4^{3-}, H_2PO^{4-} and HPO_4^{2-} released a lot of H^+; thus, the decreasing pH value can be used to estimate the content of calcium phosphate crystals (Zhu et al., 2020). The pH value of the control group dropped most rapidly (Fig. 1A). With the addition of CSPHs, the pH value decreasing rate was slower, implying that calcium phosphate crystallization was inhibited. Notably, the effects of XOS and XOS-CSPHs-TG group were superior to CSPHs, which was very close to the effect of EDTA within 10 min of the reaction, indicating that XOS-CSPHs-TG virtually prevented calcium from forming insoluble calcium phosphate. Therefore, it is vital to introduce XOS to form copolymers with CSPHs to improve the calcium-binding ability and further enhance their ability to hinder calcium phosphate crystallization.

After gastrointestinal digestion, CSPHs-Ca and XOS-CSPHs-Ca-TG released a tiny amount of calcium ions, indicating that calcium ions

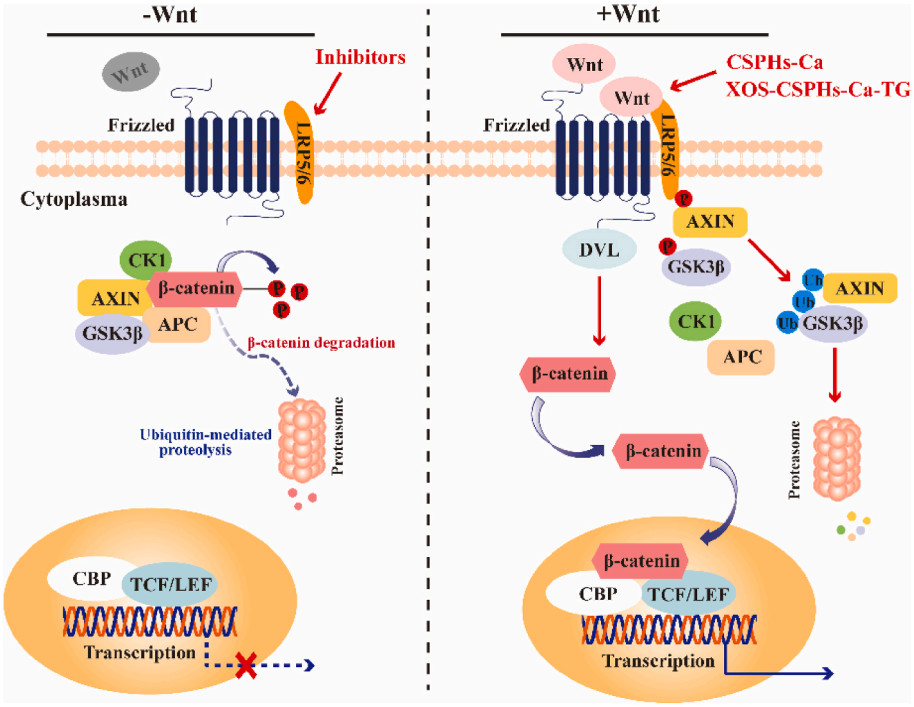

Fig. 7. Possible mechanism of CSPHs-Ca and XOS-CSPHs-Ca-TG promoting osteoblast proliferation, differentiation, and mineralization (left: inhibited; right: activated). In the presence of CSPHs-Ca and XOS-CSPHs-Ca-TG, Wnt activates the FRZ/LRP5/6 complex and subsequently promotes the expression of Dvl, therefore, leading to the phosphorylation and the degradation of the β-catenin destruction complex, including GSK-3β, APC, and AXIN. The translocation of β-catenin from the cytoplasm to the nucleus functions as a transcriptional co-activator with TCF enhancer LEF and then regulates the target genes, such as Runx2 and OPG. In the presence of the inhibitor DKK1, Wnt signals are suppressed. In the absence of the Wnt ligand, the destruction complex of β-catenin, a tertiary complex formed by AXIN, CK1, GSK3β, and APC, phosphorylates β-catenin, which subsequently undergoes the ubiquitin-proteasomal degradation.

enter the intestine in the form of soluble chelates, thereby increasing the overall absorption of calcium (Fig. 1B) (Lin et al., 2020). Similarly, Gao et al. (2018b) found that combining soluble dietary fiber (SDF) with CPP could avoid CPP degradation in the stomach and ensure that CPP bonded to calcium ions so that as many calcium ions could be absorbed in the intestine as possible.

3.2. Structural characterization

Aromatic amino acids such as tryptophan, tyrosine, and phenylalanine can generate endogenous fluorescence at specific excitation wavelengths, and the changes in fluorescence intensity can be used to study the conformational changes of peptides and their interactions with small molecules such as metal ions (Wang et al., 2021). As shown in Fig. 1C, the fluorescence intensity of CSPHs at 300–320 nm significantly decreased after being conjugated with XOS. Besides, after chelation with Ca^{2+}, the fluorescence intensity of the chelate further decreased compared to the corresponding peptides/XOS-peptides, possibly due to the formation of the peptides-Ca complex, which disrupted the conjugated double bond of CSPHs and produced substituent effect. Previous studies have shown that the chelation of metal ions with peptides can lead to endogenous fluorescence quenching, resulting from structural folding and aggregation of peptides during chelation (Cai et al., 2015; Lin et al., 2020). The decreased fluorescence intensity proved that CSPHs folded and aggregated in the glycosylation and chelation reaction with XOS and Ca^{2+}. In addition, the emerged fluorescence peak of XOS-CSPHs-Ca-TG at 400–450 nm indicated the formation of glycosylation products (Wang et al., 2021).

As shown in Fig. 1D, there were many crystal diffraction peaks in the diffraction patterns of $CaCl_2$ at certain angles, but no obvious crystal diffraction peaks were observed in the patterns of CSPHs, CSPHs-Ca, XOS-CSPHs-TG, and XOS-CSPHs-Ca-TG. Thus, it could be seen that CSPHs and XOS-CSPHs-TG were not simply mechanically mixed with $CaCl_2$ (Wang et al., 2018b). In addition, compared with CSPHs spectra, the peak positions and peak intensities of the spectra of other substances had changed significantly, indicating that new chemical complexes had been formed after glycosylation and chelation reactions (Lin et al., 2019).

As shown in Fig. 1E, CSPHs-Ca was spherical and connected precisely to form a grape cluster with a rough surface, possibly due to the cross-linking interaction effect induced by Ca^{2+} (Chen et al., 2014; Zhu et al., 2020). Moreover, XOS-CSPHs-Ca-TG was also precisely linked together, the shape was more uniform and smaller, and the surfaces became smooth, which indicated that XOS could wrap CSPHs-Ca while XOS-CSPHs-Ca-TG could be well combined through covalent bonds. Therefore, it could be confirmed that the glycosylation reaction has effectively optimized the CSPHs-Ca structure (Wu et al., 2017).

To clarify the structural changes caused by glycosylation and chelation, the FTIR spectra of the samples were compared and analyzed (Fig. 1F). The stretching vibration absorption peak of –OH and N–H is 3427.64 cm^{-1} and 2909.74 cm^{-1}, respectively, the interval of which is the characteristic peak of XOS (Sudha et al., 2011). The characteristic peaks of saccharides in XOS-CSPHs-TG and XOS-CSPHs-Ca-TG were broader and stronger than those in CSPHs and CSPHs-Ca, which indicated that different glycosylation products were formed. The stretching vibration of C═O caused amide I brand (Miller et al., 2013). After chelating with Ca^{2+}, the absorption peak of CSPHs shifted from 1653.68 cm^{-1} to 1666.70 cm^{-1}; after glycosylation, the absorption peak also shifted accordingly. Meanwhile, the absorption peak of about 1640 cm^{-1} was caused by the stretching vibration of –COO– (Wang et al., 2017). Therefore, C═O and –COO– also play an essential role in the covalent binding reaction. Moreover, compared with CSPHs-Ca and CSPHs, glycosylation products showed the shift of absorption peak and the change of intensity at 1200-1000 cm^{-1}, indicating that there were more –OH in the copolymer (Geng et al., 2014). Results showed that the TGase could bind XOS to CSPHs. It could be inferred that the amino nitrogen atom, carboxyl oxygen atom, hydroxyl, and carbonyl oxygen atom might be the primary interaction sites of CSPHs and XOS-CSPHs-TG with Ca^{2+} (Gao et al., 2018b; Lin et al., 2020; Zhu et al., 2020).

3.3. Effects on calcium absorption in Caco-2 cells

Since the chelation reaction is a rapid process, the polypeptides used in this study were premixed with calcium ions to form a chelating solution to act on the cells directly (Hobbs et al., 2001; Lin et al., 2020). As

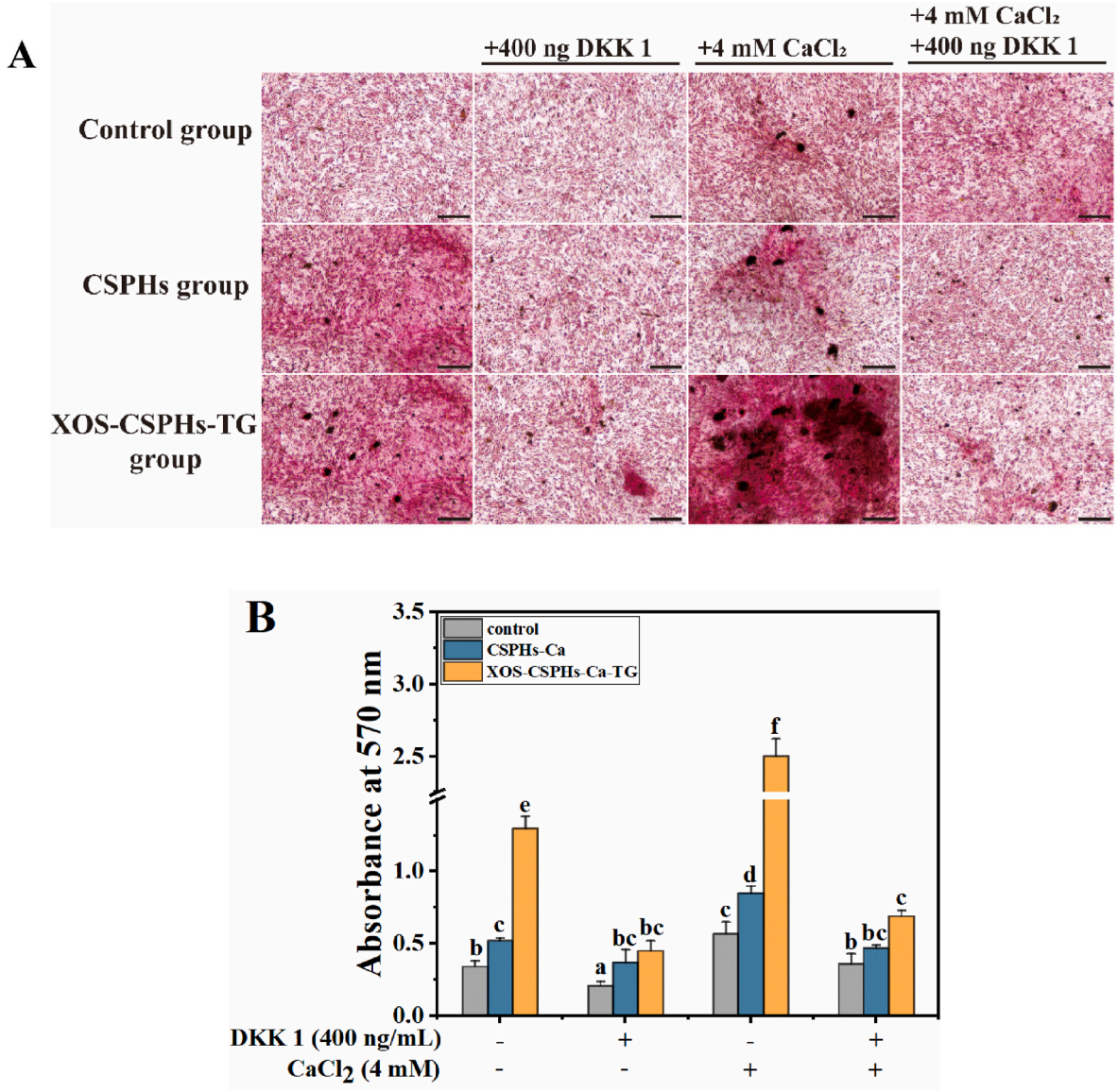

Fig. 8. Effects on mineralized nodules of MC3T3-E1 cells. (A) Alizarin red S staining. (B) Quantitative analysis. Scale bar: 100 μm. Different lowercase letters mean a significantly different, $p<0.05$. (For interpretation of the references to color in this figure legend, the reader is referred to the Web version of this article.)

shown in Fig. 2A, CSPHs-Ca and XOS-CSPHs-Ca-TG significantly improved calcium absorption in the Caco-2 cell model ($p<0.05$). Meanwhile, 8 mg/mL CSPHs-Ca and XOS-CSPHs-Ca-TG enhanced the calcium absorption by 109% and 113%, respectively, compared with the $CaCl_2$ group ($p<0.05$), and the effects of which on calcium absorption were equivalent ($p>0.05$). However, whether CSPHs-Ca and XOS-CSPHs-Ca-TG play the same role in promoting calcium absorption needs further study. Similarly, results were also found on fish scale protein hydrolysate (Lin et al., 2020), soybean hydrolysate (Lv et al., 2008), and tilapia bone collagen hydrolysate (Liao et al., 2020), indicating that calcium-chelating peptide was interacting with the plasma membrane as a calcium carrier to increase calcium influx, thus promoting calcium uptake (Hou et al., 2015; Lin et al., 2020).

The absorption of calcium ions across intestinal epithelium mainly includes two modes: paracellular transport and transcellular transport (Sun et al., 2016). When treated with 4 mg/mL and 8 mg/mL CSPHs-Ca, the calcium transport of CSPHs-Ca was 2.51 and 2.74 folds higher than that of the control group, respectively (Fig. 2B) ($p<0.05$). There was no significant difference between them ($p>0.05$), implying that the calcium transport of CSPHs-Ca was saturable. It suggests that the transcellular transport might be involved in CSPHs-Ca to facilitate calcium absorption, which contrasts with the previous reports showing that the paracellular pathway is one of the main pathways of calcium transport across Caco-2 cell monolayer in the presence of peptide-calcium chelates (Sun et al., 2016). With the increase of XOS-CSPHs-Ca-TG concentration, calcium transport increased significantly dose-dependent ($p<0.05$). While in the presence of 8 mg/mL XOS-CSPHs-Ca-TG, calcium transport was 3.54 folds higher than in the control group ($p<0.05$). Therefore, the main pathway of the XOS-CSPHs-Ca-TG encouraging calcium absorption in cell monolayer may differ from that of CSPHs-Ca, and it should be the paracellular cell pathway (Liao et al., 2020). Notably, after glycosylation, the calcium transport capacity of XOS-CSPHs-Ca-TG was remarkably higher than that of XOS and CSPHs ($p<0.05$), indicating that glycosylation is an effective means to enhance the calcium absorption of peptide-calcium chelate.

3.4. Effects on the proliferation of MC3T3-E1 cells

The proliferation process of pre-osteoblasts is the premise of forming new bone in bone tissue, which is also the critical process affecting bone

anabolism in the body (Kenichi et al., 1998). The MC3T3-E1 cells model was used to assess the osteogenic activity of peptide-calcium chelates *in vitro*. As shown in Fig. 3, the cell viability of MC3T3-E1 cells was remarkably up-regulated to about 120%–155% after being cultured for 24–72 h in CSPHs-Ca and XOS-CSPHs-Ca-TG. As shown in supplemental materials Table S2, when treated with CSPHs-Ca and XOS-CSPHs-Ca-TG, the G0/G1 phase ratio decreased immensely, while the ratio of the S phase increased ($p < 0.05$). Meanwhile, compared with CSPHs-Ca, XOS-CSPHs-Ca-TG had a more notable cell cycle stimulation effect ($p < 0.05$). Altogether, the proliferation of MC3T3-E1 cells stimulated by CSPHs-Ca and XOS-CSPHs-Ca-TG was related to the regulation of the cell cycle, which accelerated the transformation from the G0/G1 phase to the S phase, advanced DNA synthesis, and thus boosted cell proliferation (Liu et al., 2014).

3.5. Effects on ALP activity in MC3T3-E1 cells

ALP is an external enzyme of osteoblasts, and its expression activity is a remarkable feature of osteoblast differentiation (Jie et al., 2018). As shown in Fig. 4A, ALP activity of MC3T3-E1 cells treated with CSPHs-Ca and XOS-CSPHs-Ca-TG was significantly higher than that of the control group ($p < 0.05$), and the ALP activity were highest in XOS-CSPHs-Ca-TG groups. That might be because XOS-CSPHs-Ca-TG contains more hydroxyl groups after glycosylation, which could better interact with MC3T3-E1 cell surface receptors, the "external-internal signal" on MC3T3-E1 cells (Jie et al., 2018). In other words, more hydroxyl groups in XOS-CSPHs-Ca-TG enhance cell interaction and trigger signal conversion, thereby stimulating cell differentiation through receptor-mediated mechanisms (Jie et al., 2018; Liu et al., 2013). Interestingly, it takes almost 6 d for MC3T3-E1 cells to differentiate into mature osteoblasts. The ALP activity in all groups on day 14 was lower than on day 7, which might be because ALP is an early phenotypic marker during osteoblast differentiation (Wang et al., 2012). As the differentiation time is prolonged, ALP might catalyze the hydrolysis of bone phosphate monoester to provide inorganic phosphates, which bind to calcium to regulate bone metabolism and mineralization (Jie et al., 2018).

3.6. Effects on OCN and Col-I secretion in MC3T3-E1 cells

OCN and Col-I are biochemical markers of bone metabolism (Liu et al., 2017). OCN is necessary for osteoblasts to regulate the process of mineralization, and Col-I is the major protein in the bone matrix, synthesized by osteoblasts and involved in differentiation (Willett et al., 2014). After 7 d of differentiation, the secretion of OCN and Col-I in MC3T3-E1 cells treated with CSPHs-Ca and XOS-CSPHs-Ca-TG was significantly higher than that of the control group ($p < 0.05$) (Fig. 4B–C). After 14 d of differentiation, the content of OCN and Col-I in all treatment groups continued to increase concentration-dependent ($p < 0.05$). Moreover, the cells treated with XOS-CSPHs-Ca-TG had higher secretion ($p < 0.05$). It suggests that CSPHs-Ca and XOS-CSPHs-Ca-TG could enhance OCN and Col-I secretion in osteoblasts and further promote differentiation of osteoblasts in early and mature stages (Liu et al., 2017).

3.7. Effects on mRNA expression of Wnt/β-catenin pathway-related factors

The canonical Wnt signaling pathway is essential in regulating bone homeostasis, which controls the proliferation and differentiation of osteoblastic precursors and maintains mature osteoblasts (Wu et al., 2019). It was known that Wnt3a could activate the canonical Wnt signaling pathway (Ikehata et al., 2017). Wnt3a promotes Dishevelled (DVL) expression by activating the Frizzled/LRP5/6 complex, which leads to the phosphorylation and the degradation of the β-catenin destruction complex (including glycogen synthase kinase 3β (GSK-3β), adenomatous polyposis coli (APC), and Axis inhibition protein (AXIN)) (Hwang et al., 2009). Subsequently, the translocation of β-catenin from the cytoplasm to the nucleus functions as a transcriptional co-activator with T cell factor enhancer lymphoid enhancer factor (TCF/LEF) and then regulates the target genes, such as Runt-related transcription factor 2 (Runx2) and osteoprotegerin (OPG), both key transcription factors associated with the expression with osteoblast differentiation (Hwang et al., 2009; Wu et al., 2019). As shown in Fig. 5, compared to the control group, the mRNA expression of Wnt3a, LRP5, β-catenin, Runx2, and OPG was significantly increased after being treated with CSPHs-Ca and XOS-CSPHs-Ca-TG ($p < 0.05$), while the expressions level of GSK-3β was gradually inhibited dose-dependent. Meanwhile, the XOS-CSPHs-Ca-TG has a more significant effect ($p < 0.05$). That evidence strongly suggests that glycosylated peptide-calcium chelate plays a positive role in osteogenesis.

To confirm that the canonical Wnt signaling pathway is a stimulator and regulator of osteogenesis, the cells were incubated with DKK 1 (binds to LRP5/6 co-receptor and inhibits canonical Wnt/β-catenin signaling) before being treated with CSPHs-Ca and XOS-CSPHs-Ca-TG. As shown in Fig. 6, pretreatment with DKK 1 reduced ALP activity (Fig. 6A) and mRNA expression level of osteogenic transcription factor stimulated by CSPHs-Ca and XOS-CSPHs-Ca-TG to the control level (Fig. 6B–E) ($p < 0.05$). To sum up, the Wnt/β-catenin signaling pathway regulates the differentiation of MC3T3-E1 cells stimulated by CSPHs-Ca and XOS-CSPHs-Ca-TG (Fig. 7).

3.8. Effects on mineralized nodules of MC3T3-E1 cells

Mineralization is the last step of osteoblast differentiation, directly reflecting osteogenesis's degree (Jie et al., 2018). The calcium ions in the mineralized nodule are a dark red color after complexation with alizarin red S, and its absorbance is directly proportional to the amount of calcium deposition (Wu et al., 2020). Compared to the control group, both treatments in 400 μg/mL could produce a small number of mineralized nodules, while XOS-CSPHs-TG had a more significant effect ($p < 0.05$) (Fig. 8A). After adding 400 ng/mL DKK 1, the number of mineralized nodules in each treatment group decreased significantly, which was still slightly higher than that in the control group ($p < 0.05$) (Fig. 8A–B). When 4 mM $CaCl_2$ was premixed with 400 μg/mL CSPHs and XOS-CSPHs-TG to form chelates, the number of mineralized nodules increased significantly, and the XOS-CSPHs-Ca-TG had a more significant effect ($p < 0.05$) (Fig. 8B). It could be explained by the fact that the calcium-binding capacity of the XOS-CSPHs-Ca-TG was better than CSPHs-Ca (data not shown), which could provide more calcium ions and higher-density nucleation sites for the formation of minerals, leading to reduced interfacial energy generated by minerals, in turn, promote the mineralization process (Jie et al., 2018; Wu et al., 2020). Thus, CSPHs-Ca and XOS-CSPHs-Ca-TG regulate the proliferation, differentiation, and mineralization of MC3T3-E1 cells by activating the Wnt/β-catenin signaling pathway.

4. Conclusions

In this study, the structural properties and osteogenic activity of glycosylated peptide-calcium chelate were firstly investigated. Compared with CSPHs-Ca, the XOS-CSPHs-Ca-TG had better calcium phosphate crystallization inhibition activity with more unified structures. The formation of XOS-CSPHs-Ca-TG avoided digestion in the stomach and dramatically improved the calcium transport efficiency in the Caco-2 cell monolayer. Moreover, XOS-CSPHs-Ca-TG showed excellent osteogenic activity, which could effectively promote the proliferation, differentiation, and mineralization of MC3T3-E1 cells, and this beneficial effect of XOS-CSPHs-Ca-TG was achieved by activating the Wnt/β-catenin signaling pathway. Thus, XOS-CSPHs-Ca-TG plays a pivotal role in improving/preventing osteoporosis and can be used as a functional food ingredient to prevent bone metabolism-related diseases.

CRediT authorship contribution statement

Xiaoping Wu: Conceptualization, Methodology, Investigation, Formal analysis, Writing – original draft. **Fangfang Wang:** Methodology, Investigation, Formal analysis. **Xixi Cai:** Conceptualization, Methodology, Writing – review & editing, Funding acquisition. **Shaoyun Wang:** Conceptualization, Methodology, Writing – review & editing, Funding acquisition.

Declaration of competing interest

The authors declare that they have no known competing financial interests or personal relationships that could have appeared to influence the work reported in this paper.

Acknowledgements

This work was supported by National Natural Science Foundation of China (No. 31901639, 32272311), central government guided local science and technology development projects of China (No. 2020L3004), Natural Science Foundation of Fujian, China (2022J01097), and Fuzhou University Open Testing Fund of Large Precious Apparatus (2022T015).

Appendix A. Supplementary data

Supplementary data to this article can be found online at https://doi.org/10.1016/j.crfs.2022.10.008.

Abbreviations

ALP	alkaline phosphatase
APC	adenomatous polyposis coli
AXIN	adenomatous polyposis coli
CK1	casein kinase 1
Col-I	type I collagen
CSPHs	crimson snapper scales protein hydrolysates
Dvl	dishevelled
FBS	Fetal bovine serum
GSK-3β	glycogen synthase kinase 3β
HBSS	Hank's balanced salt solution
LEF	lymphoid enhancer factor
LRP5/6	LDL-receptor-related protein 5/6
OCN	osteocalcin
OPA	ortho-phthalaldehyde
OPG	osteoprotegerin
PI	propidium iodide
Runx2	Runt-related transcription factor 2
TCF	T cell factor
Tgase	transglutaminase
XOS	xylooligosaccharides
XRD	X-ray diffraction

References

Ai, T., Hao, L., Shang, L., Wang, L., Li, B., Li, J., 2021. Konjac oligosaccharides modulate the gut environment and promote bone health in calcium-deficient mice. J. Agric. Food Chem. 69, 4412–4422.

Arora, V., Singh, G., O-Sullivan, I., Ma, K., Anbazhagan, A.N., Votta-Velis, E.G., Bruce, B., Richard, R., van Wijnen, A.J., Im, H.J., 2021. Gut-microbiota modulation: the impact of the gut-microbiotaon osteoarthritis. Gene 785, 145619.

Cai, X., Zhao, L., Wang, S., Rao, P., 2015. Fabrication and characterization of the nanocomposite of whey protein hydrolysate chelated with calcium. Food Funct. 6, 816–823.

Chen, D., Mu, X., Huang, H., Nie, R., Liu, Z., Zeng, M., 2014. Isolation of a calcium-binding peptide from tilapia scale protein hydrolysate and its calcium bioavailability in rats. J. Funct. Foods 6, 575–584.

Feng, X., Dai, H., Yu, Y., Wei, Y., Tan, H., Tang, M., Ma, L., Zhang, Y., 2022. Adjusting the interfacial property and emulsifying property of cellulose nanofibrils by ultrasonic treatment combined with gelatin addition. Food Hydrocolloids 133, 107905.

Gao, A., Dong, S., Chen, Y., Chen, G., Li, S., Chen, Y., 2018a. *In vitro* evaluation and physicochemical characteristics of casein phosphopeptides-soluble dietary fibers copolymers as a novel calcium delivery system. Food Hydrocolloids 79, 482–490.

Gao, A., Dong, S., Wang, X., Li, S., Chen, Y., 2018b. Preparation, characterization and calcium release evaluation in vitro of casein phosphopeptides-soluble dietary fibers copolymers as calcium delivery system. Food Chem. 245, 262–269.

Geng, X., Cui, B., Li, Y., Jin, W., An, Y., Zhou, B., Ye, T., He, L., Liang, H., Wang, L., Chen, Y., Li, B., 2014. Preparation and characterization of ovalbumin and carboxymethyl cellulose conjugates via glycosylation. Food Hydrocolloids 37, 86–92.

Hobbs, H.A., Kendall, W.F., Darrabie, M., Opara, E.C., 2001. Prevention of morphological changes in alginate microcapsules for islet xenotransplantation. J. Invest. Med. 49, 572–575.

Hou, T., Wang, C., Ma, Z., Shi, W., Liu, W., He, H., 2015. Desalted duck egg white peptides: promotion of calcium uptake and structure characterization. J. Agric. Food Chem. 63, 8170–8176.

Hwang, I., Seo, E.Y., Ha, H., 2009. Wnt/beta-catenin signaling: a novel target for therapeutic intervention of fibrotic kidney disease. Arch Pharm. Res. (Seoul) 32, 1653–1662.

Ikehata, M., Yamada, A., Morimura, N., Itose, M., Suzawa, T.S., Shirota, T., Chikazu, D., Kamijo, R., 2017. Wnt/beta-catenin signaling activates nephronectin expression in osteoblasts. Biochem. Biophys. Res. Commun. 484, 231–234.

Jiang, B., Mine, Y., 2000. Preparation of novel functional oligophosphopeptides from hen egg yolk phosvitin. J. Agric. Food Chem. 48, 990–994.

Jie, Y., Li, Xiaoyun, Cai, Z., Ma, Meihu, Jin, Y., Ahn, D.U., Huang, X., 2018. Phosphorylation of phosvitin plays a crucial effects on the protein-induced differentiation and mineralization of osteoblastic MC3T3-E1 cells. Int. J. Biol. Macromol. 118, 1848–1854.

Kenichi, M., Katsumi, I., Yasuhiro, K., Yamori, Y., 1998. Resveratrol stimulates the proliferation and differentiation of osteoblastic MC3T3-E1 cells. Biochem. Biophys. Res. Commun. 253, 859–863.

Kim, H.K., Kim, M.G., Leem, K.H., 2008. Inhibitory effects of egg yolk soluble protein on bone resorption. Biosci., Biotechnol., Biochem. 72, 1929–1931.

Li, Y., Liu, C., Xue, W., 2012. Using response surface methodology to optimize hydrolysis of allergic protein from Mandarin fish with papain. Food Sci. (N. Y.) 33, 199–204.

Liao, W., Chen, H., Jin, W., Yang, Z., Cao, Y., Miao, J., 2020. Three newly isolated calcium-chelating peptides from tilapia bone collagen hydrolysate enhance calcium absorption activity in intestinal Caco-2 cells. J. Agric. Food Chem. 68, 2091–2098.

Lin, Y., Tang, X., Xu, L., Wang, S., 2019. Antibacterial properties and possible action mechanism of chelating peptides-zinc nanocomposite against Escherichia coli. Food Control 106, 106675.

Lin, Y., Cai, X., Wu, X., Lin, S., Wang, S., 2020. Fabrication of snapper fish scales protein hydrolysate-calcium complex and the promotion in calcium cellular uptake. J. Funct. Foods 65, 103717.

Liu, J., Czernick, D., Lin, S.C., Alasmari, A., Serge, D., Salih, E., 2013. Novel bioactivity of phosvitin in connective tissue and bone organogenesis revealed by live calvarial bone organ culture models. Dev. Biol. 381, 256–275.

Liu, J., Zhang, B., Song, Shujun, Ma, M., Si, S., Wang, Y., Xu, B., Feng, K., Wu, J., Guo, Y., 2014. Bovine collagen peptides compounds promote the proliferation and differentiation of MC3T3-E1 pre-osteoblasts. PLoS One 9, e99920.

Liu, Y., Huang, L., Hao, B., Li, H., Zhu, S., Wang, Q., Li, R., Xu, Y., Zhang, X., 2017. Use of an osteoblast overload damage model to probe the effect of icariin on the proliferation, differentiation and mineralization of MC3T3-E1 cells through the Wnt/beta-catenin signalling pathway. Cell. Physiol. Biochem. 41, 1605–1615.

Liu, G., Guo, B., Sun, S., Luo, M., Liu, F., Miao, J., Tang, J., Huang, Y., Cao, Y., Song, M., 2021. Promoting the calcium-uptake bioactivity of casein phosphopeptides *in vitro* and *in vivo*. Front. Nutr. 8, 743791.

Lv, Y., Bao, X.L., Yang, B.C., Ren, C.G., Guo, S.T., 2008. Effect of soluble soybean protein hydrolysate-calcium complexes on calcium uptake by Caco-2 cells. J. Food Sci. 73, 168–173.

Miller, L.M., Bourassa, M.W., Smith, R.J., 2013. FTIR spectroscopic imaging of protein aggregation in living cells. Biochim. Biophys. Acta 1828, 2339–2346.

Pirestani, S., Nasirpour, A., Keramat, J., Desobry, S., 2017. Preparation of chemically modified canola protein isolate with gum Arabic by means of Maillard reaction under wet-heating conditions. Carbohydr. Polym. 155, 201–207.

Sudha, T.B., Thanikaivelan, P., Ashokkumar, M., Chandrasekaran, B., 2011. Structural and thermal investigations of biomimetically grown casein-soy hybrid protein fibers. Appl. Biochem. Biotechnol. 163, 247–257.

Sun, N., Wu, H., Du, M., Tang, Y., Liu, H., Fu, Y., Zhu, B., 2016. Food protein-derived calcium chelating peptides: a review. Trends Food Sci. Technol. 58, 140–148.

Sun, X., Sarteshnizi, R.A., Boachie, R.T., Okagu, O.D., Abioye, R.O., Pfeilsticker, R.P., Ohanenye, I.C.O., Udenigwe, C.C.U., 2020. Peptide-mineral complexes: understanding their chemical interactions, bioavailability, and potential application in mitigating micronutrient deficiency. Foods 9, 1402.

Tonk, C.H., Shoushrah, S.H., Babczyk, P., El Khaldi-Hansen, B., Schulze, M., Herten, M., Tobiasch, E., 2022. Therapeutic treatments for osteoporosis-which combination of pills is the best among the bad? Int. J. Mol. Sci. 23, 1393.

Wang, W., Olson, D., Cheng, B., Guo, X., Wang, K., 2012. Sanguis Draconis resin stimulates osteoblast alkaline phosphatase activity and mineralization in MC3T3-E1 cells. J. Ethnopharmacol. 142, 168–174.

Wang, X., Gao, A., Chen, Y., Zhang, X., Li, S., Chen, Y., 2017. Preparation of cucumber seed peptide-calcium chelate by liquid state fermentation and its characterization. Food Chem. 229, 487–494.

Wang, H., Chen, N., Shen, S., Li, H., Hu, X., Yang, Y., Yu, X., Ye, L., Zhou, W., Feng, M., 2018a. Peptide TQS169 prevents osteoporosis in rats by enhancing osteogenic differentiation and calcium absorption. J. Funct.Foods 49, 113–121.
Wang, L., Ding, Y., Zhang, X., Li, Y., Wang, R., Luo, X., Li, Y., Li, J., Chen, Z., 2018b. Isolation of a novel calcium-binding peptide from wheat germ protein hydrolysates and the prediction for its mechanism of combination. Food Chem. 239, 416–426.
Wang, Z., Liu, D., Zheng, J., Xie, Y., Han, J., Wang, Y., 2021. Preparation and emulsifying properties of Maillard reaction products of soybean protein isolate under high hydrostatic pressure. Sci. Technol. Food Ind. 42, 49–58.
Willett, T.L., Pasquale, J., Grynpas, M.D., 2014. Collagen modifications in postmenopausal osteoporosis: advanced glycation endproducts may affect bone volume, structure and quality. Curr. Osteoporos. Rep. 12, 329–337.
Wu, X., Liu, Y., Liu, A., Wang, W., 2017. Improved thermal-stability and mechanical properties of type I collagen by crosslinking with casein, keratin and soy protein isolate using transglutaminase. Int. J. Biol. Macromol. 98, 292–301.
Wu, F., Jiao, J., Liu, F., Yang, Y., Zhang, S., Fang, Z., Dai, Z., Sun, Z., 2019. Hypermethylation of Frizzled1 is associated with Wnt/beta-catenin signaling inactivation in mesenchymal stem cells of patients with steroid-associated osteonecrosis. Exp. Mol. Med. 51, 1–9.
Wu, W., He, L., Li, C., Zhao, S., Liang, Y., Yang, F., Zhang, M., Jin, G., Ma, M., 2020. Phosphorylation of porcine bone collagen peptide to improve its calcium chelating capacity and its effect on promoting the proliferation, differentiation and mineralization of osteoblastic MC3T3-E1 cells. J. Funct. Foods 64, 103701.
Yamada, S., Nagaoka, H., Terajima, M., Tsuda, N., Hayashi, Y., Yamauchi, M., 2013. Effects of fish collagen peptides on collagen post-translational modifications and mineralization in an osteoblastic cell culture system. Dent. Mater. J. 32, 88–95.
Zhang, K., Li, B., Chen, Q., Zhang, Z., Zhao, X., Hou, H., 2018a. Functional calcium binding peptides from Pacific Cod (Gadus macrocephalus) bone: calcium bioavailability enhancing activity and anti-osteoporosis effects in the ovariectomy-induced osteoporosis rat model. Nutrients 10, 1–16.
Zhang, L., Lin, Y., Wang, S., 2018b. Purification of algal calcium-chelating peptide and its physical chemical properties. J. Aquat. Food Prod. Technol. 27, 518–530.
Zhang, Z., Lin, T., Meng, Y., Hu, M., Shu, L., Jiang, H., Gao, R., Ma, J., Wang, C., Zhou, X., 2021. FOS/GOS attenuates high-fat diet induced bone loss via reversing microbiota dysbiosis, high intestinal permeability and systemic inflammation in mice. Metab. Clin. Exp. 119, 154767.
Zhao, N., Hu, J., Hou, T., Ma, Z., Wang, C., He, H., 2014. Effects of desalted duck egg white peptides and their products on calcium absorption in rats. J. Funct. Foods 8, 234–242.
Zhu, B., He, H., Guo, D., Zhao, M., Hou, T., 2020. Two novel calcium delivery systems fabricated by casein phosphopeptides and chitosan oligosaccharides: preparation, characterization, and bioactive studies. Food Hydrocolloids 102, 105567.